Spatial localization of Mms6 during biomineralization of Fe_3O_4 nanocrystals in *Magnetospirillum magneticum* AMB-1

Zachery Oestreicher
School of Natural System, College of Science and Engineering, Kanazawa University, Kakuma machi, Kanazawa 920 1192, Japan; and School of Environment and Natural Resources, The Ohio State University, Columbus, Ohio 43210, USA

Eric Mumper
School of Earth Sciences, The Ohio State University, Columbus, Ohio 43210, USA

Carol Gassman
Department of Chemistry, Columbia Basin College, Pasco, Washington 99301, USA

Dennis A. Bazylinski
School of Life Sciences, University of Nevada, Las Vegas, Las Vegas, Nevada 89154, USA

Steven K. Lower
School of Earth Sciences, The Ohio State University, Columbus, Ohio 43210, USA; and School of Environment and Natural Resources, The Ohio State University, Columbus, Ohio 43210, USA

Brian H. Lower[a)]
School of Environment and Natural Resources, The Ohio State University, Columbus, Ohio 43210, USA

(Received 26 June 2015; accepted 25 January 2016)

Magnetotactic bacteria mineralize nanometer-size crystals of magnetite (Fe_3O_4) through a series of protein-mediated reactions that occur inside of organelles called magnetosomes. Mms6 is a transmembrane protein thought to play a key role in magnetite mineralization. We used both electron and fluorescent microscopy to examine the subcellular location of Mms6 protein within single cells of *Magnetospirillum magneticum* AMB-1 using Mms6-specific antibodies. We also purified magnetosomes from *M. magneticum* to determine if Mms6 was physically attached to magnetite crystals. Our results show that Mms6 proteins are present during crystal growth, and Mms6 is found in direct contact with the magnetite crystals or within the lipid/protein membrane surrounding the magnetite crystals. Mms6 was not detected at other subcellular locations within the bacteria or isolated fractions. Because Mms6 was found to completely surround the magnetosomes rather than being localized to one specific area of the magnetosome, it appears that this protein could act on the entire magnetite crystal during the biomineralization process. This supports a model in which Mms6 functions to regulate Fe_3O_4 crystal morphology. This knowledge is important for future in vitro experiments utilizing Mms6 to synthesize tailored nanomagnets with specific physical or magnetic properties.

I. INTRODUCTION

Magnetic nanoparticles hold great promise for many applications including, magnetic separations in biotechnology, delivery of cancer treatments, magnetic resonance imaging, data storage, and clean up of environmental contaminants.[1–10] Humans have therefore spent much of the past decade trying to synthesize magnetic nanoparticles with controllable size and morphology (e.g., Ref. 11). There is another organism that has spent considerably more time perfecting the art of fabricating nanometer scale magnets. A group of prokaryotes called magnetotactic bacteria (MTB) have evolved a unique set of genes to direct the biological synthesis of nanometer size, monodisperse magnets. The human quest to synthesize the ideal nanomagnet may benefit from our ability to mimic the biomineralization reaction within this single-celled organism.

MTBs use a specialized set of proteins to mineralize chemically pure, single domain, nanometer-size crystals of magnetite (Fe_3O_4) and or greigite (Fe_3S_4) under physiological conditions.[12–14] The morphology of the crystals can be elongate hexagonal, tooth/bullet-shaped, cuboctahedral, or octahedral, depending on the species of MTB. Crystal length ranges from 35 to 120 nm, which puts the magnets in the single domain size range.[15] The magnetic crystals are formed and contained within a intracellular, organelle known as the magnetosome.[16] Most MTB cells contain between 20 and 50 of these magnetosomes.[17]

Contributing Editor: Laurie Gower
[a)]Address all correspondence to this author.
e mail: Lower.30@osu.edu
DOI: 10.1557/jmr.2016.41

A major challenge to replicating the bacterial production of nano-magnetic crystals is determining which proteins are specific to MTB biomineralization and how those proteins participate in the process. Biomagnetite proteins exclusively associated with the magnetosome are named membrane specific proteins (Mam) and magnetic particle membrane specific proteins (Mms).[18–20] These proteins are encoded as a cluster of 48 genes on the highly conserved magnetosome island.[19,20] However, little is know about how these proteins get emplaced in the magnetosome membrane and the temporal arrangement of particular proteins in relation to the appearance of magnetite.[21,22]

Mms6 has been shown to be a key protein involved in the mineralization of magnetite in vivo.[23–27] Mms6 contains 59 amino acids and is 6.3 kDa in its mature state (12.5 kDa in its premature state).[23] This protein has a hydrophilic C-terminal which is tightly bound to the magnetite crystal and a membrane-bound, hydrophobic, leucine–glycine rich N-terminus.[23,24,28] The goal of this study is to determine the location of Mms6 proteins inside of individual cells of *M. magneticum* AMB-1. This has been accomplished by using two different techniques: gold immunolabeling with transmission electron microscopy (TEM) and fluorescent labeling with confocal laser scanning microscopy (CLSM).

II. MATERIALS AND METHODS

A. Purification of the protein

Mms6 was purified using the technique described by Prozorov et al.[24] Plasmids (pTrcHis-TOPO) containing the gene sequence for the mature Mms6 protein from *M. magneticum* AMB-1 and a poly His-tag on the N-terminus were used to transform XL-1 Blue Competent Cells (Stratagene, La Jolla, California). The proteins were over-expressed in the cells using IPTG induction and then purified using TALON metal affinity resin (Clontech, Mountain View, California). Most of the proteins were insoluble, so 8 M guanidine was used to solubilize the inclusion bodies. The recombinant protein was dialyzed to allow Mms6 to refold into its native state. Purified recombinant Mms6 was resolved by SDS-PAGE, stained with Coomassie Simply Blue Safe Stain (Invitrogen, Carlsbad, California) and sequenced using mass spectrometry to confirm that the correct protein was purified.

B. Mass spectrometry of recombinant protein

Mms6 protein was sequenced at The Ohio State University Mass Spectrometry and Proteomics Facility. The protein band was cut from the gel and then digested and sequenced using capillary-liquid chromatography tandem mass spectrometry (Cap-LC/MS/MS) using a Thermo Finnigan LTQ mass spectrometer equipped with a CaptiveSpray source (Bruker Michrom, Billerica, MA) operated in positive ion mode. Sequence information from the MS/MS data was processed by converting the raw data files into a merged file (.mgf) using an in-house program, RAW2MZXML n MGF batch (merge.pl, a Perl script). The resulting mgf files were searched using Mascot Daemon by Matrix Science version 2.3.2 (Boston, MA) and the database searched against the full SwissProt database version 2012 06 (536,489 sequences; 190,389,898 residues) or NCBI database version 20120515 (18,099,548 sequences; 6,208,559,787 residues). Protein identifications were checked manually and proteins with a Mascot score of 50 or higher with a minimum of two unique peptides from one protein having a -b or -y ion sequence tag of five residues or better were accepted.

C. Production of the antibody

Purified recombinant Mms6 was sent to ProSci Incorporated (Poway, CA) to produce polyclonal antibodies in rabbits. After eight weeks, the serum was removed from the rabbit and the Mms6 antibodies were purified from rabbit serum using affinity purification by attaching recombinant Mms6 to a resin and running the serum through a column containing the Mms6 resin. The final concentration of the antibody was 1.42 mg/mL as determined by direct ELISA. Pre-immune serum was removed from the rabbit before injecting the antigen (recombinant Mms6) into the rabbit which was later used as a control for immunoblotting.

D. Immunoblotting analysis

Two different amounts of recombinant Mms6 protein (0.5 and 0.05 μg) and three different cell fractions of *M. magneticum* AMB-1 were resolved by SDS using 10 well 16% Tris–glycine gels (Invitrogen). The three cell fractions and the total amount used in each lane were: (a) magnetosome membrane (10 μg), (b) cellular soluble protein (10 μg), and (c) cell membrane (10 μg). Two identical gels were run simultaneously; one gel was used for blotting, the other was imaged after staining with Simply Blue Safe Stain (Invitrogen). BenchMark prestained protein ladder (Invitrogen) was used on both gels. The proteins were blotted onto a PVDF membrane (Invitrogen), blocked with 5% BSA, labeled with the anti-Mms6 antibody at a concentration of 1:50,000 and labeled with a secondary goat anti-rabbit HRP (horseradish peroxidase) antibody at a concentration of 1:200 using the Clean-Blot IP Detection Kit HRP (Thermo-Pierce, Rockford, Illinois). The membrane was analyzed on a Gel Logic 1500 using Kodak software (Rochester, New York). As a control to test whether or not the antibody binds to Mms6, the procedure above was repeated, but 300 μg of recombinant Mms6 was added to the antibody solution.

E. Magnetosome isolation and enrichment

M. magneticum AMB-1 cells (ATCC 700264) were cultured in two 19 L carboys containing 15 L of magnetic Spirillum growth medium (ATCC medium 1653), purged with nitrogen gas for 20 min, inoculated with 250 mL of culture and allowed to grow to midlog phase. The cells were harvested and centrifuged using a continuous flow centrifuge (Heraeus 17RS, Thermo Fisher Scientific, Waltham, Massachusetts) for 1 h. The cell pellet was resuspended in 10 mM Tris–HCl pH 8.0 and the cells were lysed by passing them through a French press three times using 18,000 lb/in^2 of pressure. The magnetosomes were isolated by placing the solution in a beaker with two cobalt samarium magnets on the outside of the beaker. After 10 min the solution was poured off and replaced with fresh 10 mM Tris–HCl. This was repeated 11 more times after which the magnetosomes were suspended in 10 mM Tris–HCl. An aliquot of this final suspension was used to separate the magnetite crystals from the membranes by incubating the magnetosomes in 10 mM Tris–HCl with 1% SDS for 3 h. The solution was centrifuged at 12,000 × *g* for 20 min and the supernatant containing only magnetosome membrane was removed. The absence of magnetite in this fraction was checked using TEM.

F. Cell fractionation

The solution from the first magnetosome isolation step (above) was used to isolate the cell membrane fraction and the soluble protein fraction by centrifugation at 200,000 × *g* at 4 °C for 3 h. The supernatant (containing the soluble proteins) was removed and the pellet (containing the cell membrane fraction) was resuspended in 10 mM Tris–HCl.

G. Embedding and labeling with immunogold

Magnetospirillum magneticum AMB-1 were cultured in a 1 L Schott bottle using the formula for magnetic Spirillum growth medium (ATCC medium 1653). The sealed bottles were purged with nitrogen gas for 30 min before autoclaving. After autoclaving the bottles were inoculated with *M. magneticum* AMB-1 and grown at 28 °C until they reached midlog phase, after which they were processed for TEM.

We followed the protocol of Taoka et al. for the labeling experiments.[29] The cells were pelleted at 10,000 × *g* for 10 min and then washed with 0.1 M sodium cacodylate, fixed in 3% paraformaldehyde/0.1% glutaraldehyde, dehydrated in a graded ethanol series, and embedded using LR white medium grade resin (EMS, Electron Microscopy Sciences, Hatfield, Pennsylvania) in 00 gelatin capsules and cured at 60 °C for 24 h. Sections (60 nm in thickness) were cut from one of the blocks and placed on formvar and carbon coated nickel slot grids (Ted Pella, Redding, California). The sections were allowed to dry on the grids for several hours to overnight before being immunolabeled. The grids were floated on drops of 0.1 M glycine in Tris–HCl for 20 min, then blocked with 0.1% cold water fish gelatin, 1% BSA, 0.1% Tween-20, in Tris–HCl for 30 min. The grids were incubated overnight at 4 °C on a drop of Mms6 antibody diluted 1:2000 in 0.5% BSA Tris–HCl. The grids were washed with Tris–HCl with 1% BSA and incubated on drops of goat anti-rabbit IgG antibody conjugated with 10 nm gold (Sigma-Aldrich, St. Louis, Missouri) diluted 1:100 in 0.5% BSA in Tris–HCl for 2 h. This size of gold particles is between the 5 and 15 nm diameter particles used by Taoka et al., 2006 to label Mam proteins in a different MTB species, *M. magnetotacticum* MS-1.[29] The grids were rinsed in Tris buffer followed by distilled water, and analyzed using an FEI Spirit TEM at 80 keV spot size 2 and imaged using a Gatan camera. No adjustments were made to the image after acquisition other than cropping in Adobe Photoshop.

Carbon-formvar 200 mesh nickel grids (Ted Pella) were placed on drops of purified magnetosomes that were diluted 1:1250 for 5 min and then rinsed in water for 15 min. The grids were then blocked with 5% BSA–Tris–HCl and incubated with the anti-Mms6 diluted 1:4000 in 0.5% BSA–Tris HCl for 8 h at room temperature. Samples were blocked again in 1% BSA–Tris–HCl and incubated with goat anti-rabbit IgG antibody conjugated with 10 nm colloidal gold (Sigma-Aldrich) diluted 1:100 in 0.5% BSA in Tris–HCl for 8 h at room temperature. After washing the grids in TBS–HCl and water, they were analyzed using an FEI Spirit (FEI Company, Hillsboro, Oregon) at 80 keV spot size 2 and imaged using a Gatan camera. No adjustments were made to the image after acquisition other than cropping in Adobe Photoshop.

H. Fluorescence CLSM

Whole, intact cells were examined using CLSM coupled with Nomarski imaging. *M. magneticum* AMB-1 cells were grown using the formula for magnetic Spirillum growth medium (ATCC medium 1653) in 125 mL serum bottles containing 55 mL media with nitrogen gas in the headspace. Once the cells had reached midlog phase, they were harvested by centrifuging at 10,000 × *g* for 10 min at 4 °C and the cell pellet was fixed in 4% paraformaldehyde for 5 min. The cells were centrifuged again at 8000 rpm for 10 min and the cell pellet was suspended in water. A drop of cells was placed on a slide and allowed to air dry. The slide was washed with PBS (phosphate buffered saline, pH 7.4), labeled with primary antibody (1:400) for 1 h, washed with PBS, labeled with a secondary antibody, goat anti-rabbit IgG anti-body conjugated to Dylight 488 (1:100) (Thermo Fisher Scientific) and washed with PBS and water. The cells were analyzed using an Olympus FluoView 1000; no adjustment was made to the images after acquisition other than cropping in Adobe Photoshop.

I. Transmission electron microscopy

Whole, intact isolated magnetosomes were analyzed as well as ultrathin sections of AMB-1 cells. The whole cell is not visible in these TEM images due to the thinness of the sections. The chain of magnetosomes can be clipped in these TEM images because of the oblique slice of the section.

The samples were tagged with polyclonal antibodies that were made specifically to target Mms6 epitopes. These were used as a primary antibody, which attach directly to Mms6 proteins. This was followed by labeling with a secondary antibody, which has affinity for the primary antibody. The secondary antibody has a marker conjugated to it, which makes it visible in the microscope. In the case of the CLSM (see above), the secondary antibody contains a fluorophore. For TEM, the marker was a 10 nm gold sphere. The gold marker appears as an opaque sphere in the micrograph at the site of the protein.

III. RESULTS

A. Recombinant protein rMms6 purification

The His-tagged, recombinant Mms6 (rMms6) protein was purified using TALON metal affinity resin that had been charged with Co^{2+}. Fractions from the purification protocol were resolved using SDS-PAGE [Fig. 1]. The fractions eluted from the TALON column were dominated by a polypeptide with a mass of approximately 13 kDa [Fig. 1], which corresponded to the expected size of rMms6. These fractions also contain minor amounts of other protein bands [Fig. 1]. The major 13 kDa protein band [shown with an arrow in Fig. 1] was excised and sequenced by mass spectrometry. This band was determined to be the magnetite particle specific iron-binding protein Mms6.

B. Western blot analysis using anti-Mms6 antibody

Protein fractions isolated from *M. magneticum* AMB-1 were resolved by SDS-PAGE and stained with Coomassie to visualize the proteins contained within the different fractions [Fig. 2]. The cell membrane, soluble, and magnetosome membrane fractions show several Coomassie-stained bands [Fig. 2]. In particular, the magnetosome membrane fraction [Fig. 2, lane 4] exhibits faint banding between 15 and 6 kDa, which corresponds to the expected size of Mms6. There is no obvious banding less than 37 kDa in the soluble protein fraction [Fig. 2, lane 3].

Proteins contained within the cell membrane, soluble, and magnetosome membrane fractions were resolved using SDS-PAGE and transferred to a PVDF membrane for immunoblot analysis [Fig. 3(a)]. The cell membrane

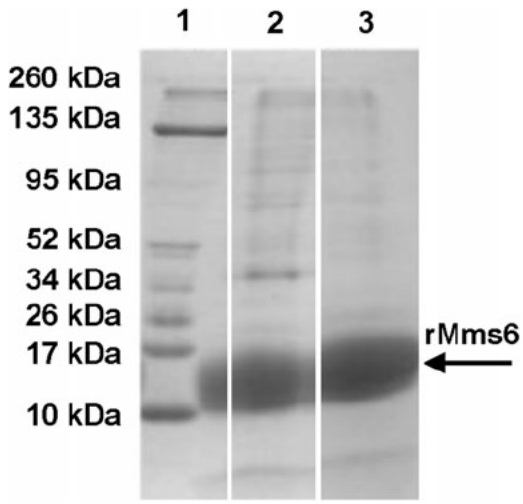

FIG. 1. Different fractions from the purification of rMms6, resolved using SDS PAGE, transferred to PVDF and stained with Coomassie. Lane 1 shows the positions and molecular masses (in kilodaltons) of the protein standards. Lane 2 is 10 μg of the protein fraction that was loaded onto the TALON (Clontech Labs) column charged with cobalt. Lane 3 contains 10 μg of the protein fraction that was eluted from the Co^{2+} column using 300 mM imidazole. The black arrow shows the excised band confirmed to be the recombinant protein Mms6 (rMms6) via mass spectrometry.

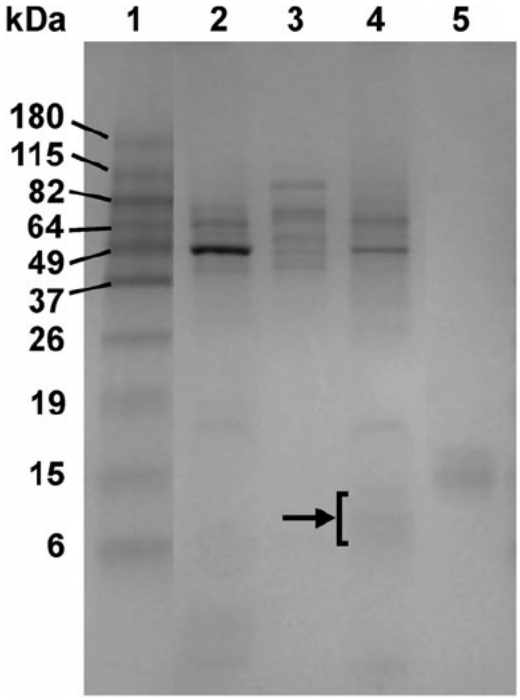

FIG. 2. Coomassie stained SDS PAGE showing the protein and cell fractions from *Magnetospirillum magneticum* AMB 1 used to test the affinity of the Mms6 antibody in the protein immunoblot. Lane 1 shows the positions and molecular masses (in kilodaltons) of the protein standards. Lane 2 is cell membrane (10 μg). Lane 3 is soluble protein (10 μg). Lane 4 is magnetosome membrane (10 μg). The faint protein bands between 15 and 6 kDa correspond to the expected size of Mms6 and is marked with a black arrow and bracket. Lane 5 contains 0.5 μg of purified recombinant Mms6.

[Fig. 3(a), lane 1] and soluble protein [Fig. 3(a), lane 2] fractions displayed no obvious banding between 6 and 19 kDa, which was the expected size-range for Mms6. The lane containing the magnetosome membrane fraction [Fig. 3(a), lane 3] contained a single polypeptide band at approximately 11 kDa that bound to anti-Mms6. While no band was observed in the lane containing 0.05 µg of purified recombinant Mms6 [Fig. 3(a), lane 4], several prominent polypeptide bands were observed in the lane containing 10-times more rMms6 [Fig. 3(a), lane 5]. The anti-Mms6 labeling was primarily observed as a double band at approximately 16 kDa and two additional faint bands at approximately 37 and 49 kDa [Fig. 3(a), lane 5]. In the control immunoblot [Fig. 3(b)], excess rMms6 protein was added to the antibody to ensure that anti-Mms6 was binding to Mms6 and not labeling other polypeptides within the cell fractions. No polypeptide bands were observed on this Western blot [Fig. 3(b)].

C. CLSM analysis

The specific location of Mms6 molecules within intact cells was determined using CLSM on *M. magneticum* AMB-1 cells labeled with anti-Mms6 antibodies. Figure 4 shows fluorescently labeled *M. magneticum* AMB-1 cells. In Figures 4(b) and 4(a) distinct line of features is seen on the cells. These linear "bumps" correspond to the magnetosome chain running along the length of individual bacteria. Figure 4(a) shows the merged Nomarski image (black and white) and fluorescent image (green areas) demonstrating Mms6-labeling in the center, along the major axis of the cell, corresponding to the position of the magnetosome chain within each bacterium.

No Mms6 labeling occurred distal to the major axis of the cell [Fig. 4]. That is, there was no clear labeling on the cell membrane, the cytosol, or the surface of the

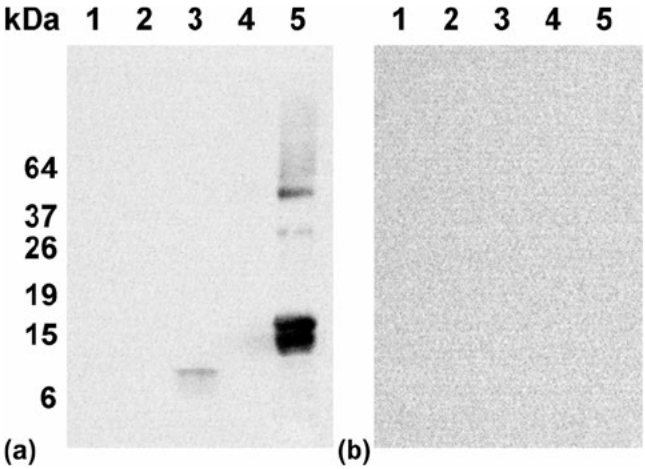

FIG. 3. Western immunoblot analysis. (a) Immunoblot analysis of rMms6 protein and three different cell fractions from *Magnetospirillum magneticum* AMB 1. (b) The same immunoblot as (a) except that 300 µg of recombinant Mms6 was added to the antibody mixture as a control. Lane 1 is cell membrane (10 µg). Lane 2 is soluble protein (10 µg). Lane 3 is magnetosome membrane (10 µg). Lane 4 contains 0.05 µg of purified recombinant Mms6. Lane 5 contains 0.5 µg of recombinant Mms6. The positions and molecular masses (in kilodaltons) of the protein standards are also shown to the left.

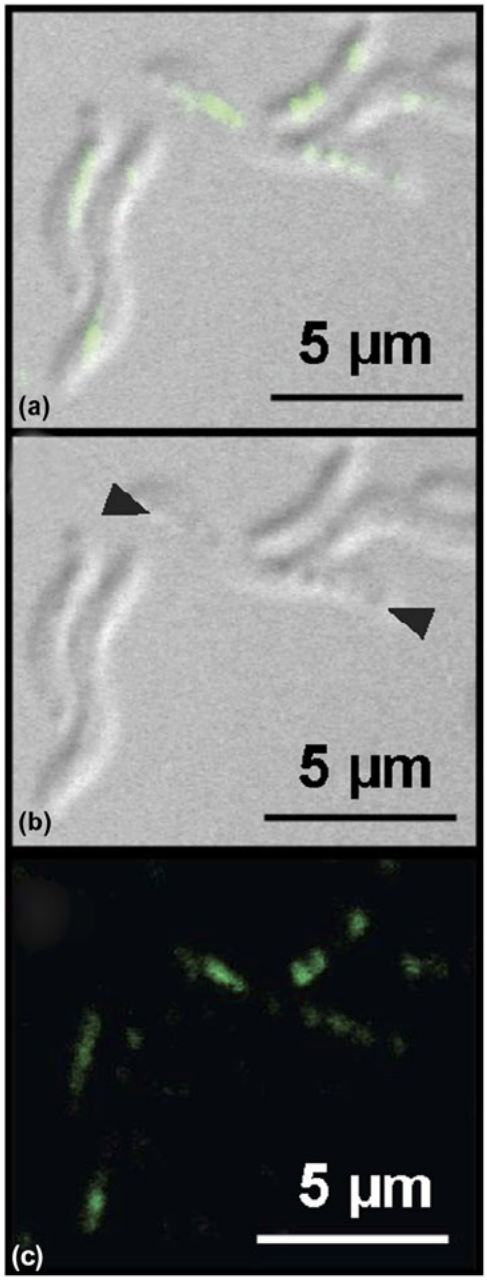

FIG. 4. Fluorescently labeled *Magnetospirillum magneticum* AMB 1 cells using anti Mms6 (1:400) as the primary antibody and goat anti rabbit Dylight 488 (1:100) as the secondary. (a) Merged Nomarski and fluorescent images showing the outline of *M. magneticum* cells with the fluorescent tag localized to the middle of the cells. (b) The same field of view as (a), using only Nomarski microscopy. The magneto some chain for one bacterium can been seen running between two black arrowheads. (c) The same field of view as (a), showing only the fluorescent image. Scale bar in all panels is 5 µm.

bacteria. A negative control was also prepared to confirm that the results were not due to background labeling by the secondary antibody. The control slide (not shown) did not contain any fluorescently labeled cells.

D. TEM analysis

Two different samples were analyzed using TEM: (i) 60 nm thick, ultra-thin sections of *M. magneticum* AMB-1 and (ii) purified chains of magnetosomes isolated from *M. magneticum* AMB-1. Figure 5(a) shows that the cells displayed Mms6-labeling adjacent to the magnetosomes, either directly touching the Fe_3O_4 crystal or within the organic matrix surrounding the magnetosome. Labeling did not occur on all the magnetosomes, which may have been a consequence of the sectioning process. Importantly, Mms6-labeling was observed mainly on the magnetosomes and rarely on other parts of the cell [Fig. 5(a)].

Control experiments were performed to confirm the specificity of the Mms6-antibody and gold label in the TEM images. Figure 5(b) is labeled the same as the thin section shown in Fig. 5(a), with the exception that the primary antibody (i.e., anti-Mms6) was substituted with 0.5% BSA–Tris–HCl. The sample shown in Fig. 5(c) was prepared the same as Fig. 5(a), except that the primary antibody (i.e., anti-Mms6) was substituted with 5% pre-immune serum from the rabbit that was used to produce the antibodies. This pre-immune serum should not contain any of the antibodies for Mms6. Indeed no gold labels were detected in TEM images prepared from these control experiments [Figs. 5(b) and 5(c)].

TEM was also used to analyze chains of magnetosomes isolated from *M. magneticum* AMB-1 cells [Fig. 6]. The magnetosomes were labeled with the same primary antibody (i.e., anti-Mms6) and the same gold-conjugated secondary antibodies that were used with the thin sections shown in Fig. 5. We observed numerous nanogold particles coating the purified magnetosomes [Fig. 6(a)]. The nanogold particles were observed either in direct contact with the Fe_3O_4 crystal or within the magnetosome membrane that surrounded the Fe_3O_4 [Fig. 6(a) inset]. Figures 6(b) and 6(c) are negative controls, performed like the controls used with the cell thin sections described above. Figure 6(b) was prepared exactly as Fig. 6(a), except with 0.5% BSA–Tris–HCl

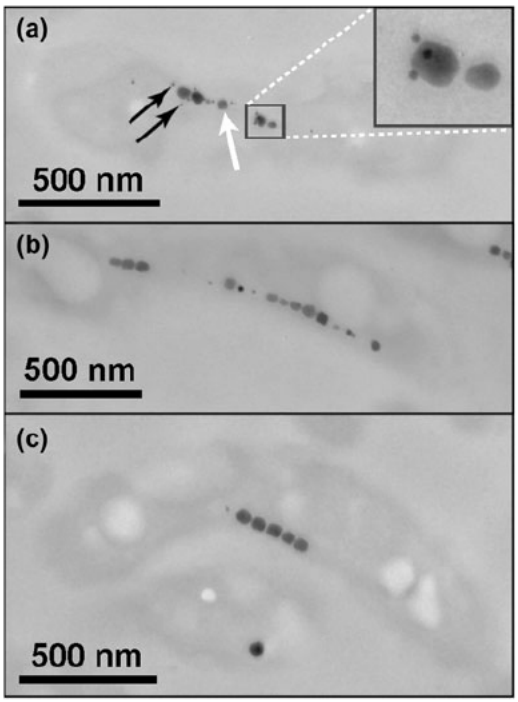

FIG. 5. Ultrathin sections of *Magnetospirillum magneticum* AMB 1. (a) A single cell showing magnetosomes (solid white arrow) labeled with primary antibody anti Mms6 (1:2000) and then secondarily labeled with goat anti rabbit antibody conjugated to 10 nm colloidal gold (black arrows). Inset shows a detail of two of the magnetosomes. (b) Negative control for the immunolabeling showing an ultrathin section treated exactly the same as the ultrathin section in (a), but substituting 0.5% BSA Tris HCl for the primary antibody. (c) A second type of negative control for the immunolabeling treated exactly the same as the section in (a), but with 5% pre immune serum substituted for the primary antibody. Scale bars are 500 nm.

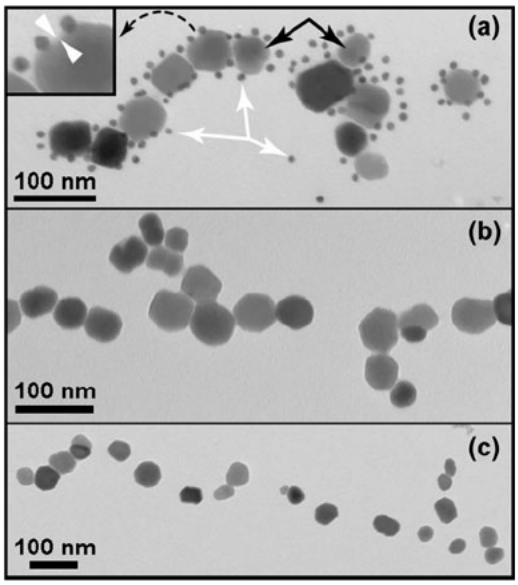

FIG. 6. Purified magnetosomes from *Magnetospirillum magneticum* AMB 1. (a) Magnetosomes (solid black arrows) labeled with primary antibody anti Mms6 (1:4000) and secondarily labeled with goat anti rabbit antibody conjugated to 10 nm colloidal gold (solid white arrows). The inset in (a) shows a single magnetite crystal labeled with gold conjugated Mms6 antibody. The space between the white arrow heads shown in inset depicts the magnetosome membrane. (b) Negative control for the immunolabeling experiment treated exactly the same as (a), except substituting 0.5% BSA Tris HCl for the primary antibody. (c) Negative control treated exactly the same way as (a), but substituting 5% pre immune rabbit serum in place of the primary antibody. Scale bars are 100 nm.

substituted for the primary antibody (i.e., anti-Mms6). Figure 6(c) was prepared exactly as Fig. 6(a), however, the primary antibody (i.e., anti-Mms6) was substituted with 5% pre-immune serum. No nanogold labeling was observed for either of these control experiments [Figs. 6(b) and 6(c)].

IV. DISCUSSION

Mms6 is one of the critical proteins involved in the synthesis of magnetite by several species of MTB. In vivo studies demonstrate that wild type *M. magnetotacticum* AMB-1 produces magnetite crystals with [100] and [111] faces, but magnetite crystals produced in Δ*mms*6 AMB-1 were smaller with a significantly different morphology.[27] In vitro experiments also support the hypothesis that Mms6 plays a key role in magnetite biomineralization. For example, other work suggest that Mms6 may preferentially interact with the [100] crystal face of magnetite.[30] Mms6 has also been used in cell-free, mineralization experiments of magnetite,[24,28] and a synthetic peptide based on Mms6 has been implicated in binding to iron and magnetite crystals.[25,27] Recently, it has been proposed that there is a suite of Mms proteins that act congruently to form a mature crystal having a specific morphology.[31] Additional research suggests that Mms6 proteins self assemble to bring together iron ions for crystal nucleation.[32,33]

Most of these past studies of Mms6 have focused on determining its function through approaches such as proteomics, genetic mutations, or iron binding experiments. These previous studies have proposed models involving the localization of various magnetosome-specific proteins during the mineralization process. However, none of them have actually demonstrated the localization of Mms6 inside of single cells. Previous work involving the localization of proteins in MTB is limited to two studies, which confirmed the location of Mam22 (MamA) and Mam12 (MamC) in *M. magnetospirillum* MC-1(Ref. 29) and MamC in *M. marinus* MC-1 (Ref. 34). The goal of this study was to elucidate the spatial arrangement of Mms6 proteins inside of individual cells of *M. magneticum* AMB-1 by using two different techniques: gold immunolabeling with TEM and fluorescent labeling with CLSM.

CLSM showed fluorescently-labeled Mms6 molecules occurring along the major axis of the cell, either intermittently or in a linear cluster. This signal was co-localized with the chain of magnetosomes in a bacterium [Fig. 4(a)]. Similarly, nanogold labeling of isolated magnetosomes clearly showed Mms6 directly adjacent to the Fe_3O_4 nanoparticles [Fig. 6(a)]. On occasion, we did notice nanogold particles that were not in direct contact with the Fe_3O_4 crystal [Figs. 5(a) and 6(a)]. This could have been caused by the inaccessibility of the protein epitope to the antibody. Alternatively, we could have disrupted the integrity of magnetosome membrane during the preparation process, thus dispersing Mms6 epitopes and causing the labeling to occur at positions not immediately adjacent to the Fe_3O_4 crystal. Nonetheless, in the vast majority of images nanogold labeling occurs directly adjacent to the magnetosomes [Figs. 5(a) and 6(a)].

An interesting observation was that not all magnetosomes were labeled in the microscopy images [e.g., Fig. 5(a)]. On the thin sections, this could be because the epitope was not exposed at the surface of the section. But in the fluorescent image, where the label is accessible to the whole cell, there should be labeling on all of the magnetosomes if Mms6 is present on each and every one of the magnetosomes. The same is true for the isolated magnetosomes [Fig. 6(a)] where the whole magnetosome is exposed to the antibody. The absence of uniform labeling of magnetosomes implies that Mms6 is only expressed during a specific time of mineral growth (as opposed to nucleation). This is consistent with the observation of Tanaka et al.[27] who showed that Mms6 is not involved in the Fe_3O_4 nucleation process. Tanaka et al.[27] were unable to determined whether Mms6 functions in subsequent stages of mineral growth.

Protein immunoblot analysis [Fig. 3] indicates that significant amounts of Mms6 are contained solely within the magnetosome membrane of *M. magneticum* AMB-1 [lane 3, Fig. 3(a)]. Mms6 was absent from the cell membrane and cytosol fractions [lanes 1 and 2, Fig. 3(a)]. Similarly, no Mms6-labeling was observed on the cell membrane of whole bacteria [Fig. 5]. Previous studies have shown that the magnetosome membrane is actually an invagination of the cell membrane that forms around each nascent magnetosome.[35,36] The fact that Mms6 was not associated with the cell membrane, either within a whole bacterium [Fig. 5] or cell membrane fraction [Fig. 3], suggests that Mms6 molecules become emplaced in the magnetosomes after the magnetosome membrane invaginates from the cell membrane. This adds credibility to the hypothesis that Mms6 has a specific "life-cycle" within the bacteria and that the Mms6 functions to control the shape and/or size of the growing Fe_3O_4 nanocrystals.[25,27,30] Perhaps, the Mms6 molecules are inserted into and removed from the magnetosome membrane at different times during the mineralization process. This could be tested in future time-point experiments where thin sections are analyzed from cells in different growth phases.

There is a significant amount of labeling of Mms6 on the isolated magnetosomes [Fig. 6(a)]. However, there is some non-uniformity to the gold labeling around each individual magnetosome. Some magnetosomes have multiple gold labels while others have very few. This could be due to the randomness of the labeling technique, the size of the gold particles, blocking of the labeling site

by another protein that associates with Mms6, or the result of actual uneven distribution of Mms6 epitopes on the magnetosomes. If the latter is the case, then labeling is occurring because the protein is present in higher concentrations on some magnetosomes. This suggests that the Mms6 is actively controlling the morphology of growing magnetite crystals. Conversely, the absence of label suggests that the crystal has finished growing.

Some of the first reports of Mms6 described the protein as being involved in crystal nucleation.[23,24,32,33] However, these examinations have all been done in vitro using isolated proteins.[23,24] Indeed, the ability of isolated Mms6 proteins to nucleate magnetite crystals has been convincingly demonstrated.[27,31] Still, the in vivo function of Mms6 within a bacterium may be to control the growth and mineralization process inside the magnetosome. The results of our localization experiments support this idea. Further, our results match the conceptual model proposed by Lohße et al., 2014.[37] Their work illustrates a temporal model of magnetosome biosynthesis in which Mms6 is only present during the "crystal maturation" stage. We observed Mms labeling only when a mature Fe_3O_4 crystal was present. Furthermore, in their model,[37] Mms6 is not present during the late "crystal maturation" stage, nor is the protein present during the final stage of "magnetosome chain assembly and positioning", both consistent with the work presented herein.

The significance of understanding magnetite biomineralization in MTB is critical if one wants to mimic MTB's capacity to biomineralize single domain magnets with uniform morphology. Previous studies have shown that Mms6 plays a strong role in shaping the magnetite crystals, but the location and timing of the activity of Mms6 during the biomineralization has not been discussed. Our results suggest that Mms6 is present during the process of mineral growth, which helps to understand the timing of the proteins' activity within MTB. This needs to be confirmed with additional time-point experiments (e.g., determine if gold nanoparticles are largely associated with mature magnetosomes as opposed to immature or empty magnetosomes from iron-limited cells). This knowledge is important for future studies, which would use Mms6 to synthesize customized magnets having a specific morphology and size. Individually tailored magnets could have many uses ranging from drug delivery in the human body to technological applications involving magnetic data storage and even strategies for environmental remediation.

ACKNOWLEDGMENTS

This research was supported by the U.S. National Science Foundation grants EAR1424138 and EAR1423939. We would like to thank Marit Nilsen-Hamilton and Pierre Palo for providing us with the plasmid used in this study and their assistance with protein purification; Sara Cole and Richard Montione at The Ohio State University Campus Microscopy and Imaging Facility for their assistance with the microscopy; and Todd Matulnik for assisting us with the batch culturing of *M. magneticum* AMB-1.

REFERENCES

1. P. Tartaj, M.P. Morales, T. Gonzalez Carreno, S. Veintemillas Verdaguer, and C.J. Serna: Advances in magnetic nanoparticles for biotechnology applications. *J. Magn. Magn. Mater.* **290**, 28 (2005).
2. T. Matsunaga and A. Arakaki: Molecular bioengineering of bacterial magnetic particles for biotechnological applications. In *Magnetoreception and Magnetosomes in Bacteria*, D. Schuler ed.; Springer: New York, 2007; p. 227 254.
3. T. Prozorov, P. Palo, L. Wang, M. Nilsen Hamilton, D. Jones, D. Orr, S.K. Mallapragada, B. Narasimhan, P.C. Canfield, and R. Prozorov: Cobalt ferrite nanocrystals: Out performing magneto tactic bacteria. *ACS Nano* **1**, 228 (2007).
4. Y. Deng, D. Qi, C. Deng, X. Zhang, and D. Zhao: Super paramagnetic high magnetization microspheres with an Fe_3O_4 SiO_2 core and perpendicularly aligned mesoporous SiO_2 shell for removal of microcystins. *J. Am. Chem. Soc.* **130**, 28 (2008).
5. J. Lee, Y. Lee, J.K. Youn, H. Bin Na, T. Yu, H. Kim, S. Lee, Y. Koo, J.H. Kwak, H.G. Park, H.N. Chang, M. Hwang, J. Park, J. Kim, and T. Hyeon: Simple synthesis of functionalized super paramagnetic magnetite/silica core/shell nanoparticles and their application as magnetically separable high performance biocatalysts. *Small* **4**, 143 (2008).
6. Y. Wang, Y.W. Ng, Y. Chen, B. Shuter, J. Yi, J. Ding, S. Wang, and S. Feng: Formulation of superparamagnetic iron oxides by nanoparticles of biodegradable polymers for magnetic resonance Imaging. *Adv. Funct. Mater.* **18**, 308 (2008).
7. M. Tanaka, A. Arakaki, S.S. Staniland, and T. Matsunaga: Simultaneously discrete biomineralization of magnetite and tellu rium nanocrystals in magnetotactic bacteria. *Appl. Environ. Microbiol.* **76**, 5526 (2010).
8. Y. Tang, D. Wang, C. Zhou, W. Ma, Y. Zhang, B. Liu, and S. Zhang: Bacterial magnetic particles as a novel and efficient gene vaccine delivery system. *Gene Ther.* **19**, 1187 (2012).
9. H.S. Huangand and J.F. Hainfeld: Intravenous magnetic nano particle cancer hyperthermia. *Int. J. Nanomed.* **8**, 2521 (2013).
10. S.C.N. Tangand and I.M.C. Lo: Magnetic nanoparticles: Essential factors for sustainable environmental applications. *Water Res.* **47**, 2613 (2013).
11. L. Li, J. Ding, and J. Xue: A facile green approach for synthesizing monodisperse magnetite nanoparticles. *J. Mater. Res.* **25**, 810 (2010).
12. R.B. Frankel, R.P. Blakemore, and R.S. Wolfe: Magnetite in freshwater magnetotactic bacteria. *Science* **203**, 1355 (1979).
13. D.L. Balkwill, D. Maratea, and R.P. Blakemore: Ultrastructure of a magnetotactic spirillum. *J. Bacteriol.* **141**, 1399 (1980).
14. B.R. Heywood, D.A. Bazylinski, A. Garrattreed, S. Mann, and R.B. Frankel: Controlled biosynthesis of greigite (Fe_3S_4) in magnetotactic bacteria. *Naturwissenschaften* **77**, 536 (1990).
15. D.A. Bazylinski and R.B. Frankel: Magnetosome formation in prokaryotes. *Nat. Rev. Microbiol.* **2**, 217 (2004).
16. D. Murat, A. Quinlan, H. Vali, and A. Komeili: Comprehensive genetic dissection of the magnetosome gene island reveals the step wise assembly of a prokaryotic organelle. *Proc. Natl. Acad. Sci. U. S. A* **107**, 5593 (2010).
17. M. Naresh, V. Hasija, M. Sharma, and A. Mittal: Synthesis of cellular organelles containing nano magnets stunts growth of magnetotactic bacteria. *J. Nanosci. Nanotechnol.* **10**, 4135 (2010).

18. M. Greenberg, K. Canter, I. Mahler, and A. Tornheim: Observa tion of magnetoreceptive behavior in a multicellular magnetotactic prokaryote in higher than geomagnetic fields. *Biophys. J.* **88**, 1496 (2005).
19. S. Ullrich, M. Kube, S. Schubbe, R. Reinhardt, and D. Schuler: A hypervariable 130 kilobase genomic region of *Magnetospirillum gryphiswaldense* comprises a magnetosome island which under goes frequent rearrangements during stationary growth. *J. Bacteriol.* **187**, 7176 (2005).
20. T. Matsunaga, Y. Okamura, Y. Fukuda, A.T. Wahyudi, Y. Murase, and H. Takeyama: Complete genome sequence of the facultative anaerobic magnetotactic bacterium *Magnetospirillum* sp strain AMB 1. *DNA Res.* **12**, 157 (2005).
21. A. Komeili, H. Vali, T.J. Beveridge, and D.K. Newman: Magneto some vesicles are present before magnetite formation, and MamA is required for their activation. *Proc. Natl. Acad. Sci. U. S. A.* **101**, 3839 (2004).
22. C.T. Lefevreand and L. Wu: Evolution of the bacterial organelle responsible for magnetotaxis. *Trends Microbiol.* **21**, 534 (2013).
23. A. Arakaki, J. Webb, and T. Matsunaga: A novel protein tightly bound to bacterial magnetic particles in *Magnetospirillum magnet icum* strain AMB 1. *J. Biol. Chem.* **278**, 8745 (2003).
24. T. Prozorov, S.K. Mallapragada, B. Narasimhan, L. Wang, P. Palo, M. Nilsen Hamilton, T.J. Williams, D.A. Bazylinski, R. Prozorov, and P.C. Canfield: Protein mediated synthesis of uniform superparamagnetic magnetite nanocrystals. *Adv. Funct. Mater.* **17**, 951 (2007).
25. A. Arakaki, F. Masuda, Y. Amemiya, T. Tanaka, and T. Matsunaga: Control of the morphology and size of magnetite particles with peptides mimicking the Mms6 protein from mag netotactic bacteria. *J. Colloid Interface Sci.* **343**, 65 (2010).
26. J.M. Galloway, A. Arakaki, F. Masuda, T. Tanaka, T. Matsunaga, and S.S. Staniland: Magnetic bacterial protein Mms6 controls morphology, crystallinity and magnetism of cobalt doped magne tite nanoparticles in vitro. *J. Mater. Chem.* **21**, 15244 (2011).
27. M. Tanaka, E. Mazuyama, A. Arakaki, and T. Matsunaga: Mms6 protein regulates crystal morphology during nano sized magnetite biomineralization in vivo. *J. Biol. Chem.* **286**, 6386 (2011).
28. S. Feng, L. Wang, P. Palo, X. Liu, S.K. Mallapragada, and M. Nilsen Hamilton: Integrated self assembly of the Mms6 magnetosome protein to form an iron responsive structure. *Int. J. Mol. Sci.* **14**, 14594 (2013).
29. A. Taoka, R. Asada, H. Sasaki, K. Anzawa, L F. Wu, and Y. Fukumori: Spatial localizations of Mam22 and Mam12 in the magnetosomes of *Magnetospirillum magnetotacticum*. *J. Bacteriol.* **188**, 3805 (2006).
30. Y. Amemiya, A. Arakaki, S.S. Staniland, T. Tanaka, and T. Matsunaga: Controlled formation of magnetite crystal by partial oxidation of ferrous hydroxide in the presence of recombinant magnetotactic bacterial protein Mms6. *Biomaterials* **28**, 5381 (2007).
31. A. Arakaki, A. Yamagishi, A. Fukuyo, M. Tanaka, and T. Matsunaga: Co ordinated functions of Mms proteins define the surface structure of cubo octahedral magnetite crystals in magnetotactic bacteria. *Mol. Microbiol.* **93**, 554 (2014).
32. L. Wang, T. Prozorov, P.E. Palo, X. Liu, D. Vaknin, R. Prozorov, S. Mallapragada, and M. Nilsen Hamilton: Self assembly and biphasic iron binding characteristics of Mms6, a bacterial protein that promotes the formation of superparamagnetic magnetite nanoparticles of uniform size and shape. *Biomacromolecules* **13**, 98 (2012).
33. W. Wang, W. Bu, L. Wang, P.E. Palo, S. Mallapragada, M. Nilsen Hamilton, and D. Vaknin: Interfacial properties and iron binding to bacterial proteins that promote the growth of magnetite nanocrystals: X ray reflectivity and surface spectroscopy studies. *Langmuir* **28**, 4274 (2012).
34. C. Valverde Tercedor, F. Abadía Molina, M. Martinez Bueno, E. Pineda Molina, L. Chen, Z. Oestreicher, B.H. Lower, S.K. Lower, D.A. Bazylinski, and C. Jimenez Lopez: Subcellular localization of the magnetosome protein MamC in the marine magnetotactic bacterium *Magnetococcus marinus* strain MC 1 using immunoelec tron microscopy. *Arch. Microbiol.* **196**, 481 (2014).
35. M. Richter, M. Kube, D.A. Bazylinski, T. Lombardot, F.O. Gloeckner, R. Reinhardt, and D. Schueler: Comparative genome analysis of four magnetotactic bacteria reveals a complex set of group specific genes implicated in magnetosome biominer alization and function. *J. Bacteriol.* **189**, 4899 (2007).
36. A. Komeili, Z. Li, D.K. Newman, and G.J. Jensen: Magnetosomes are cell membrane invaginations organized by the actin like protein MamK. *Science* **311**, 242 (2006).
37. A. Lohße, S. Borg, O. Raschdorf, I. Kolinko, É. Tompa, M. Pósfai, D. Faivre, J. Baumgartner, and D. Schüler: Genetic dissection of the *mamAB* and *mms6* operons reveals a gene set essential for magnetosome biogenesis in *Magnetospirillum gryphiswaldense*. *J. Bacteriol.* **196**, 2658 (2014).